行政院國家科學委員會補助專題研究計畫成果報告

※※※※※※※※※※※※※※※※※※※※※※※※※※
※　　　　　　　　　　　　　　　　　　　　　　　　※
※　　高速船舶艏結構碰撞破壞之研究(2/3)　　※
※　　　　　　　　　　　　　　　　　　　　　　　　※
※※※※※※※※※※※※※※※※※※※※※※※※※※

計畫類別：☑個別型計畫　　□整合型計畫
計畫編號：NSC89－2611－E－002－005
執行期間：88 年 8 月 1 日至 89 年 7 月 31 日

計畫主持人：李雅榮
計畫參與人員：張長根 曾祥達 黃建樺

本成果報告包括以下應繳交之附件：
□赴國外出差或研習心得報告一份
□赴大陸地區出差或研習心得報告一份
☑出席國際學術會議心得報告及發表之論文各一份
□國際合作研究計畫國外研究報告書一份

執行單位：台大造船及海洋工程學研究所

中　華　民　國　八十九年　八月　十五日

行政院國家科學委員會專題研究計劃第二年度成果報告

高速船舶艏結構碰撞破壞之研究(2/3)

On the Study of Collision Failure of High Speed Ship's Bow Structure

計畫編號：NSC89-2611-E-002-005

執行期限：88 年 8 月 1 日至 89 年 7 月 31 日

主持人：李雅榮(台大造船及海洋工程學研究所)

計畫參與人員: 張長根 曾祥達 黃建樺(台大造船及海洋工程學研究所)

一、摘要

在第一年度報告中，我們建立了艏結構元件受軸向碰撞衝擊時之漸進式挫曲理論分析模式。結構元件 L 形、X 形(十字形)、T 形元件的理論模型之正確性直接或間接地獲證。本報告則是延續既有的成果將理論模型推導至船艏結構的壓潰力分析。

本篇報告將 Yang & Caldwell 與 Hideomi Ohtsub 的理論基礎加以改良並應用於船艏結構的壓潰分析；兩者皆源自於 Wierzbicki 的基本崩壞模式。將船艏的結構分割成 L 形、X 形、T 形元件的組成，並將各元件所吸收的能量疊加，可得整個船艏結構的抗壓能力。鋼材艏結構已有實驗文獻可參考比較，然而鋁合金船艏則尚無文獻可比，有待下一年度的實驗計劃。此外，數值分析與理論推導結果則是相當令人滿意的吻合。

關鍵詞：艏結構碰撞、鋁合金、LS-DYNA

Abstract

Progressive buckling model of bow structural element due to axially impact load was studied and compared with numerical calculation results in the 1st report. And the validity of formula of L shape, T shape, and + shape are proved. The purpose of this report is to present a basis of the collision forces of simplified aluminium and steel bow structures.

In this paper, the Yang & Caldwell's technique as well as Hideomi Ohtsubo's technique of deriving simplified equation of mean crushing force based on the Wierzbicki's collapse mechanism is used and applied to the ship bow structures. The ship bow structure is divided into simple elements of L shape, T shape, and + shape. The absorbed energy of each elements are summed up to be the total absorbed energy in the crushing of the bow structure. The finite element analysis using LS-DYNA is applied to verify the validity of this approach. The comparisons are made with experiments by Hagiwara et al. But there is no experiment data yet of aluminium bow structures to compare with our work. The good agreements are met between the results of numerical analysis and mathematical simplified equations.

壓潰應力針對不同的細長比繪圖如下圖四:

(3)X 形基本元件(參考圖三)

X1: $E_{X1} = 8E_a + E_b + E_c + E_f + E_g$

X2: $E_{X2} = 8E_a + 4E_d + 2E_e$

X3: $E_{X3} = 8E_a + 4E_h + 4E_i$

壓潰應力針對不同的細長比繪圖如下圖五:

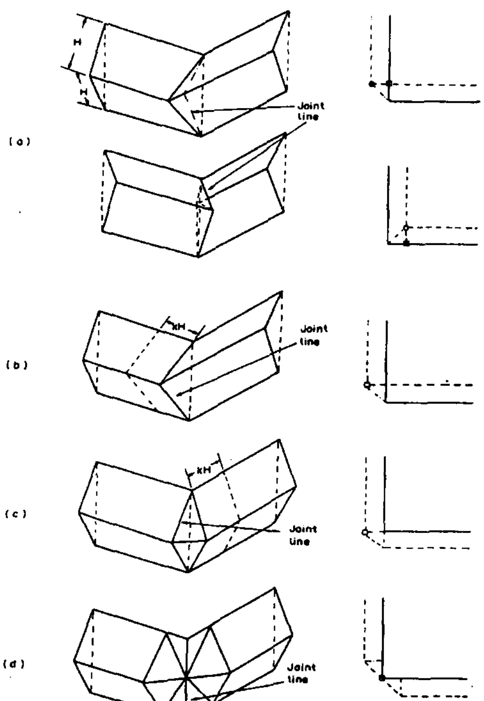

<圖一>L 形元件示意圖

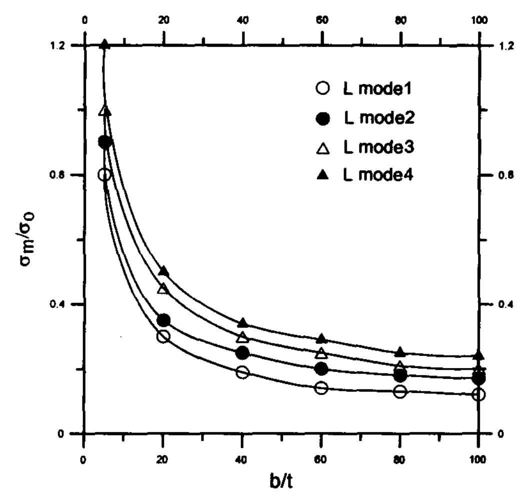

<圖二>L 形元件壓潰應力

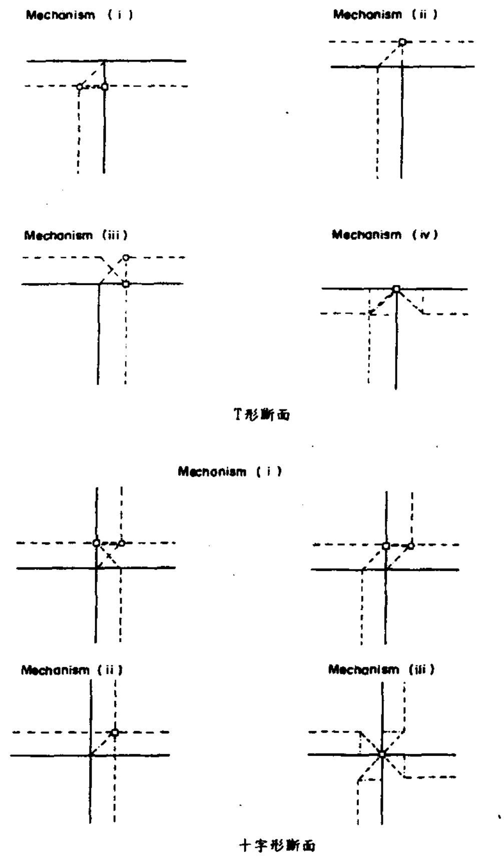

<圖三>T 形 X 形元件示意圖

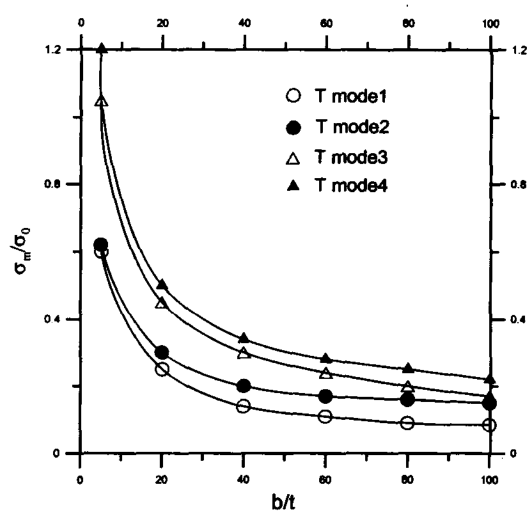

<圖四>T 形元件壓潰應力

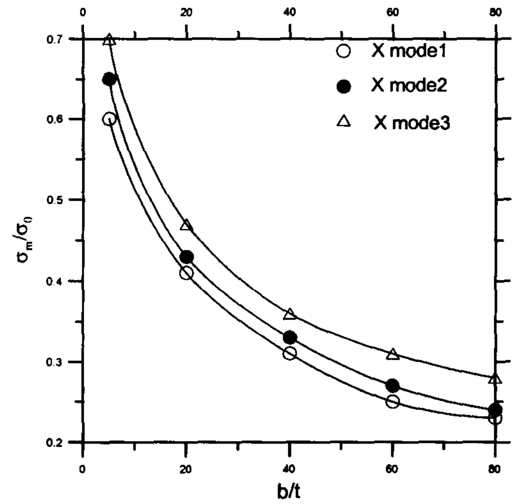

<圖五> X 形元件壓潰應力

(4)田字形複合斷面

介紹完三種基本元件，接下來對於較複雜的斷面可將其切割成既有之基本元件，以一田字形斷面為例，斷面尺寸如圖六與表一所示:

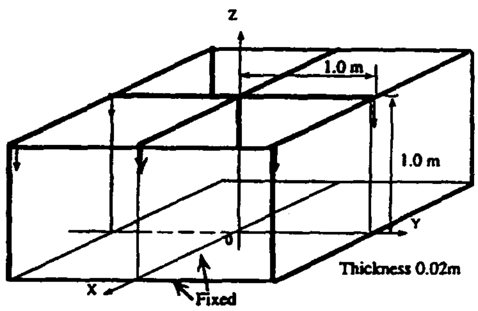

<圖六>複合斷面尺寸圖

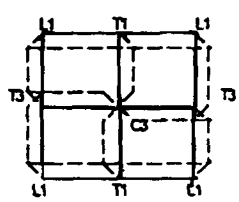

<圖七>幾何連續條件

分割方式必須考慮幾何條件之連續，並找到最小能量的組合(如圖七)，並非隨意分割。計算結果此田字形段面(鋁合金材質)在受到向下速度為 1000mm/sec 時之壓潰力為 1.51×10^6 kg。以數值方法評估後發現相當正確，容後述。

表一

楊式彈性係數 E	7150(kg/mm^2)
包松比 ν	0.34
密度 ρ	2.7x10^{-6}(kg/mm^3)
Flow stress σ_0	26(kg/mm^2)
* σ_0=(σ y+σ u)/2	
velocity=-10mm/sec ~ -1000mm/sec	

(5) 簡化之船艏結構

為更進一步驗證簡化公式的合理性，建立一箱型多層結構以模擬簡化之船艏結構，同樣地按照各 frame 分割成基本元件，並計算其壓潰力。結果顯示第一個 frame 平均壓潰力為 260000kg，第二個 frame 之平均壓潰力則為 330000kg，與數值方法比較後發現相當吻合。

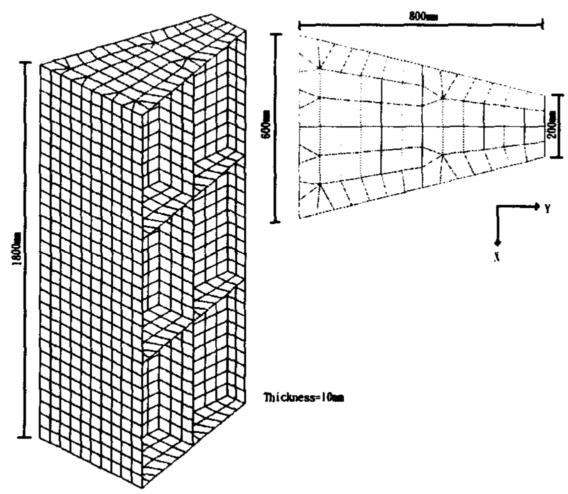

<圖八>簡化船艏結構之尺寸

(6) 與 Hagiwara 實驗模型比較

Hagiwara 在 1983 年進行一系列縮小模型實驗，建立了一艘 1:5，17000 DWT 的鋼結構船艏模型，如圖九所示，由於目前為止仍無鋁合金模型試驗，故只能與鋼材質理論模型相比較。實驗進行以擬靜態(v=0.1mm/s)進行，故可不考慮 strain-rate 效應。

Plate thickness (mm)

Stringer and decks inside	1·8
Upper deck	2·0
Side shell	2·3
Bottom plate	4·5
Stringers and plate at center	1·8

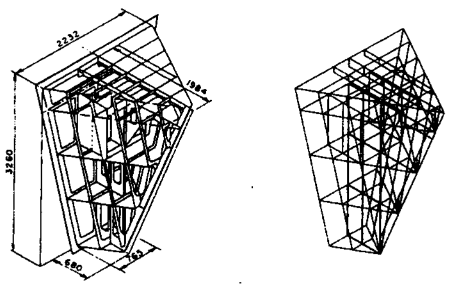

The model tested by Hagiwara and present computed model.

<圖九>Hagiwara model test

計算步驟同前，將模型分為六段 frame，一一計算各段 frame 之壓潰力。結果亦相當吻合，如圖十所示。

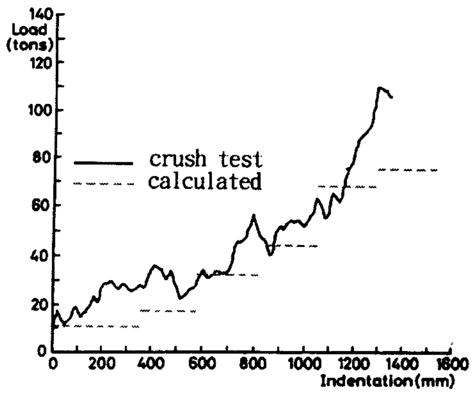

<圖十>簡化式結果與實驗結果比較

四、數值解析

(1) 田字形複合結構壓潰分析

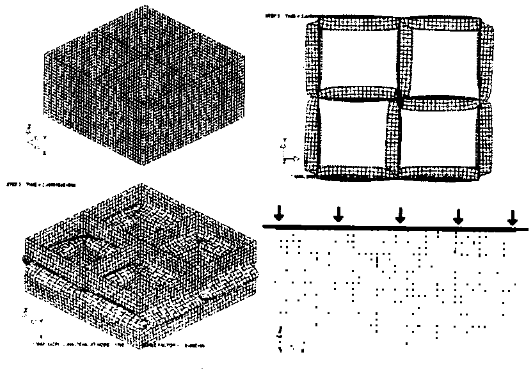

<圖十一>複合結構壓潰過程

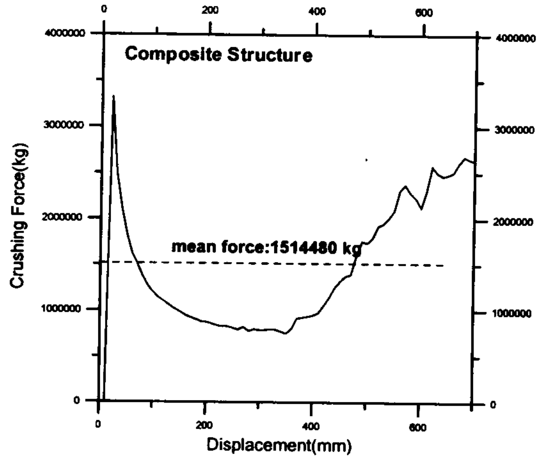

<圖十二>複合結構有限元素計算與簡化式比較

如圖十一與十二所示，LS-DYNA 計算之平均壓潰力(1514480 kg)與簡化式(1.51×10^6kg)所預測之結果一致。

(2) 簡化之船艏結構

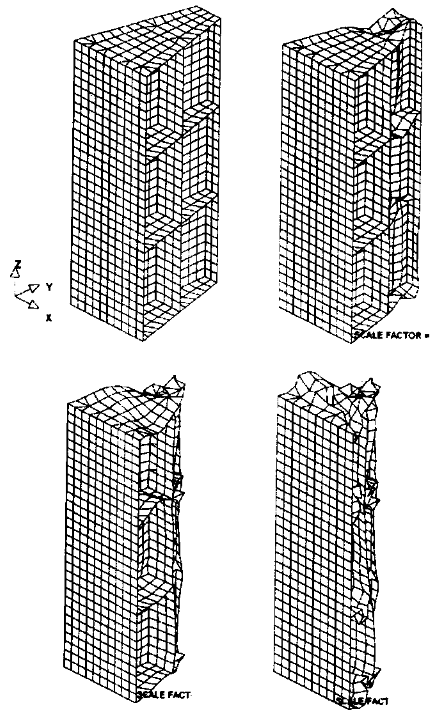

<圖十三>簡化之船艏結構壓潰過程

從圖十三、圖十四可比較得知 LS-DYNA 之計算結果($2.7\text{x}10^5$kg / $3.2\text{x}10^5$kg)與吾人之簡算式($2.6\text{x}10^5$kg / $3.3\text{x}10^5$kg)結果一致。

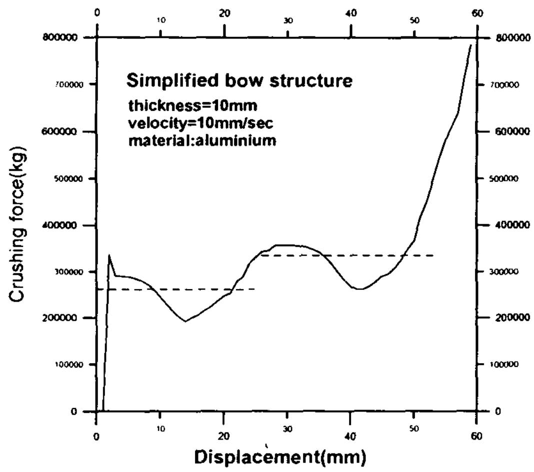

<圖十四>有限元素計算與簡化法比較

五、結語

由基本元件著手切割複雜船艏結構，簡化了計算艏結構抗壓強度的程序;目前已充分掌握鋁合金基本元件之力學與塑性行為特性，可著手於艏結構的構造分解與快速設計，以達艏結構於高速碰撞下仍保持安全航行之目的。待下年度船艏模型的建立與實驗，可使分析更臻健全。

六、參考文獻

1. J. Amdahl,"Energy absorption in ship-platform impacts", Dr.Ing.Thesis, Report No.UR-83-84,The Norwegian Institute of Technology, Trondheim, 1983.
2. P.D.C. Yang and J.B.Caldwell, "Colllsion energy absorption of ship's bow structure",Int.J.Impact Engng, 7(2), 1988.
3. H.Kierkegaard,"Ship bow response in high energy collision",Marine Structure, 6(4),1993.
4. P.Terndrup Pedersen, S.Valsgard, D.Olsen, S.Spangenberg, "Ship impact : bow collisions" ,Int.J.Impact Engng, 13(2) ,1993.
5. 大坪英臣、鈴木克幸,"The crushing mechanics of bow structure in head on collision",1st report, Tr.SNAME, Japan No.176,1994.
6. 王革、鈴木克幸、大坪英臣 "The crushing mechanics of bow structure in head on collision",2nd report, Tr. SNAME, Japan No.177,1995.
7. Martin J. Petersen, "Dynamics of ship collisions", Ocean Engng, 9(4),1982.
8. Oi-Hyun Kim, Lck-Hung Choe, Jae-Hyun Kim, Joon-Mo choug, "Bow collision analysis of high speed passenger craft", Fast l997.
9. 大西登喜夫、川上肇、安川度、長澤準,"On the ultimate strength of bow construction", Tr. SNAME, Japan No.151, 1982.
10. K.Hagiwara, H.Takanabe, H. Kawano, "A proposed method of predicting ship collision damage", Int. J. Impact Engng, 1(3), 1983.
11. H.Nagasawa, K.Arita, M.Tani, S.Oka, "A study on the collapse of ship structure in colllslon with bridge piers, J. SNAJ, 1977.
12. V.U.Minorsky, "An Analysis of Ship Collisions With Reference to Protection of Nuclear Power Plants.",J. Ship Research, 1959.
13. A.Otubushin,"Detailed Validatio of a Non-linear Finite Element Code Using Dynamic Axial Crushing of a Square Tube.",Int. J. Impact Engng. Vol.21, No 5. pp.349-368,1998.

出席 ICCE/7 心得報告

本次會議是由 International Community for Composites Engineering and College of Engineering, University of New Orleans 主辦，其目的在為材料科學、材料力學、複合材料力學、以及複合材料製程間建立聯繫管道，同時整合跨學科的航太科技、生化、電子、流體、與自動控制等。本人所著〝Analysis of the Post-Buckling Behavior of Composite Laminates Connected by Rivets〞為 500 多篇發表論文之一。

會議是在美國科羅拉多州丹佛市之 Adam's Mark Hotel 舉行，會期一共七天，自 2000 年 7 月 2 日至 8 日。本人的論文被安排於第二天 7 月 3 日發表，在抵達後即開始積極做各項準備。研討會分別在六個場地同時進行，所以必須針對個人有興趣的題目而穿梭於各場地間。從早上 8 點半開始一直到晚上九點都有議程進行，一整天下來，雖然感到疲憊，但也收穫良多。每天的第一場演講，多由大師級學者擔任，深入淺出地介紹各專題之發展及關鍵問題，7 月 5 日更安排一個 workshop，邀請政府相關部門的人員，說明政府對複合材料發展之期許，使參加之學者能瞭解政府部門之需求，達成產、官、學、研交流之目的。本人所發表的論文，也在 7 月 3 日按預定的時間順利進行。也許因為發表的場次是晚上最後一場，經過一天的勞累，出席的人數並不如白天場次那麼踴躍，但本人發表後也獲得一些學者的回應，在熱烈的討論中，獲得不少的建議與啟發，獲益良多。另外，也攜帶一些資料回國，如會議的論文集，其他學者的論文等。其中能直接與各國學者做深入討論，更是此次會議中一大收穫。

另外值得一提的是 7 月 5 日晚上，大會主席許大衛先生宴請與會的所有華人，讓來自世界各地的華人能夠藉此交流。會中台灣清華大學巢慶成教授代表台灣與會學者致贈「華人之光」金牌一面，以表達對許主席的謝意。許主席致力於推動 ICCE 年會，至今已進入第七屆，對複合材料研究的貢獻卓著，正可說是「華人之光」。晚宴中世界各地的華人齊聚一堂，在主辦單位的安排下進行各種聯誼活動，可謂賓主盡歡。

藉由此次會議中，能夠將國內之研究成果發揚於外，並吸取國外優秀研究方法，提升研發能力，確實收穫不少。期望未來能將所得應用於研究，對國內複合材料工程有所貢獻。

Analysis of the Post-Buckling Behavior of Composite Laminates Connected by Rivets

Y. J. Lee, H. J. Lin and C. C. Lin
Department of Naval Architecture and Ocean Engineering,
National Taiwan University, Taipei , Taiwan, R.O.C.

ABSTRACT

In order to reduce the calculation time, the rivets are replaced with springs in the present study, while the stiffness of the spring is induced from the analysis of the bending behavior and the interaction between the rivet and the laminate. The validity of this method is verified by experiments. Then the spring is applied on several cases, like the span between the stiffeners and the curvature of the plate. In all these cases, springs can fully present the behavior around the rivets.

KEY WORDS: Composite Materials, Post-Buckling, Rivet

1. INTRODUCTION

Composite material have been widely used in airplanes, ships, automobiles and various industries for its high specific strength, rigidity and corrosion resistance. Welding is not possible for composite laminates, so the rivets are the most frequently used to connect the composite laminates. When the laminate is fastened by the rivets, the behavior around the joint is rather complicated. The weakness of the connection usually results in total failure of the structure.

Since 1970s, there have been several research studies reported regarding this subject, however, most investigations restricted the analysis to 2D problem with a simple geometry. Ref [1] is one of the few researches that investigated on 3D finite element analysis.

Ref. [2] investigated the failure process and pin-bearing strength of laminated composites. However, in addition to planar tension, buckling caused by planar compression is even more important. Therefore, 3D analysis is imperative because the inter-laminar strength has great influence over the behavior. Few studies, like Ref. [3]~[5], analyze about the strength behavior of composite laminates with hole under buckling. While Ref. [6]~[7] conducted analysis on the buckling behavior of laminates jointed by several rivets. In these studies, the rivets are only modeled as elastic nodes instead of an elastic body. However, studies demonstrate that failure appears around the rivet. Modeling rivets with linear elastic spring is not sufficient to modify the behavior around the rivet. Ref. [8] uses the finite element software, ABAQUS, and modeled the rivets as an elastic body. Wherein the contact pressure and the stress distribution of the structure can be obtained.

In order to investigate the post buckling behavior of the laminate jointed by rivets, the finite element software ABAQUS is used in the present research. However, due to the complication of the stress around the rivet, it requires a finer mesh to appropriately present the behavior, which is time consuming and needs more calculation on the computer. In order to solve this problem, rivets are replaced with springs to present the mechanic behavior around the rivets.

The stiffness of the springs is obtained from a precisely meshed local model as in Ref[8], then the spring is used in a roughly meshed global model. Thus, the calculation time and the amount for the whole structure is reduced.

2. SIMULATION

2.1 Simulation Process Fig.1 presents a composite laminate is joined with metal stiffener by rivets. The area surrounded by dashed lines in Fig 1-2 is extracted as the local model to be analyzed. In the first step, the local model is meshed with 3D solid element, as in Fig.2, contact and failure of material are considered to simulate the nonlinear behavior around the rivets.

The second step, another local model roughly meshed with shell element is established, as shown in Fig.3, the rivet is replaced with 3 nonlinear springs in X, Y, and Z direction. The dimension and material of these two models are the same.

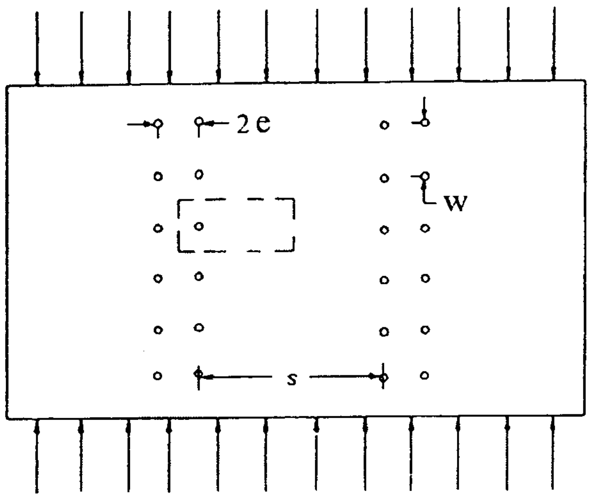

Fig.1

Then nonlinear springs are located to make this model have the same rigidity as the former (same deflection on one end under the same force), the procedure will be illustrated later. As a result, we can use the nonlinear spring to represent the mechanic behavior around the rivet.

Finally, the whole structure is meshed with shell element, thereafter rivets are replaced with nonlinear springs, then the post-buckling behavior can be analyzed efficiently.

2.2 Failure Criteria Failure behavior is considered in the simulation model. A subroutine is used to modify the values of the engineering constants and the stresses of the failed material, and calculate the new stiffness matrix. Therefore, when the material is damaged, the subroutine fixes the stiffness matrix to modify the failure.

In order to predict the final collapse behavior of the structure and make the springs contain the failure behavior, the fiber and matrix failure is considered in local model. The Hashin [9] Criterion is used to determine different types of failure. Four types of failure are considered in the present study: fiber failure in tension/compression and matrix failure in tension/compression.

When fiber breakage occurs, the longitudinal Young's modulus E_1, poison ratio v_{12}, v_{21}, v_{13}, v_{31}, shear modulus G_{12}, G_{13}, and stresses σ_{11} , τ_{12} , τ_{13} are set to zero. When the matrix cracking occurs, the transverse Young's moduli E_2, poisson's ratio v_{12}, v_{21}, v_{23}, v_{32}, shear moduli G_{12}, G_{23}, and stresses σ_{22} , τ_{12} , τ_{23} are set to zero. These types of failure leads to property degradation and reduction of the global stiffness that can induce structure collapse. Note that in 2D shell element, the Z-direction is not considered.

2.3 LOCAL ANALYSIS

2.3.1 3D Solid Element Model The material of the model is T300/976, the engineering constants of the lamina are shown in Table 1. The rivets and the stiffeners are made of aluminum alloy, the Young's modulus is 70 GPa and the Possion ratio is 0.32.

replacing the rivet is signed with springs.

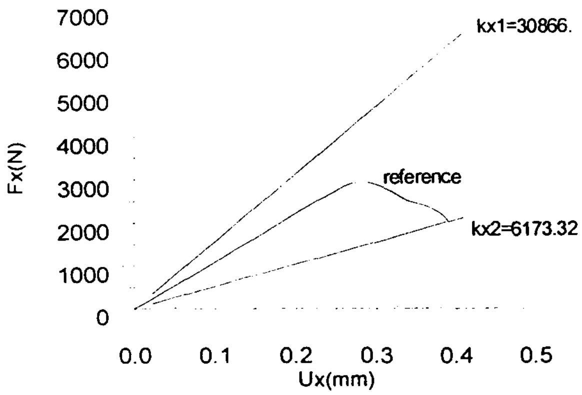

Fig.4

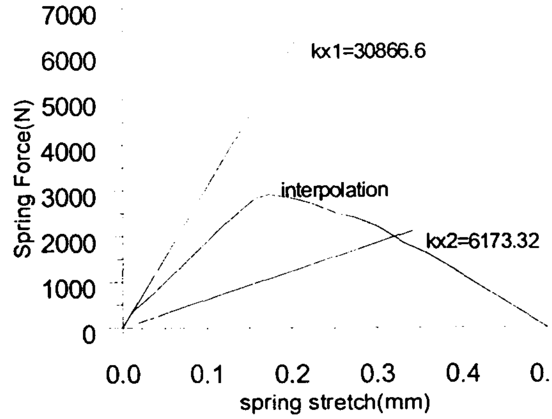

Fig.5

The stiffness of the spring is determined by the following way. First, the stiffness of the spring is given as k1. The right end of the model is forced to deflect, the displacement-force curve is called as curve-I (shown in Fig.4), while the spring is stretched at the same time. The spring force-stretch curve is called as curve-i (shown in Fig.5). Thereafter the stiffness is set as k2, then again we have the displacement -force curve-II (shown in Fig.4) and the spring force-stretch curve-ii (shown in Fig.5). According to the relation of the reference curve(the solid line in Fig.4, obtained from 3D model), curve-I, and curve-II, interpolate curve-i and curve-ii to get the stiffness curve of the spring replacing rivets. The solid line in Fig.5 is the force-stretch curve obtained from interpolation.

The force and the stretch of the spring are interpolated as follows:

$$f = \frac{RF - RF2}{RF1 - RF2}(f1 - f2) + f2 \quad , \quad e = \frac{RF1 - RF}{RF1 - RF2}(e2 - e1) + e1 \qquad (1)$$

Wherein "f" is the spring force, and "e" is stretch of the spring replacing rivets. When the deflection is "u" (as in Fig.4), the acting force in the reference curve is "RF" the acting force in curve-I is "RF1", whereas the acting force in curve-II is "RF2". Under the same displacement "u", the spring force in curve-i is "f1", the spring force in curve-ii is "f2", whereas the stretch of spring in curve-i is "e1", and the stretch of spring in curve-ii is "e2"

The interpolation (or extrapolation) is applied in X、Y、Z direction and get x, y, z three springs. By replacing the rivet with the above spring in the local model, we have a deflection-force curve as shown in Fig.6. The curve is very close to the result of 3D solid model. The same interpolation is done for Y 、 Z spring, the deflection-force curve of simplified shell model is also very close to the result of 3D solid model. That indicates this method works well for the local model, the spring can replace the mechanic behavior near the rivet.

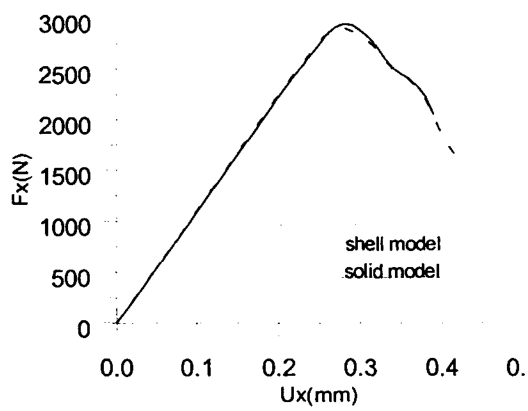

Fig.6

Through the force-stretch curve of the spring, some behavior near the rivet can be seen. The curve is almost linear at first, that means the material around the rivet is not damaged. As the stretch grows, the slop of the curve becomes smaller and smaller then the curve start to decrease after the top point. The slop of the curve decreases because the material around the rivet is damaged. This helps us to judge whether the laminate is damaged or not. If the stretch of the spring is larger than the top point, then we know that the failure appears near the rivet. It is useful when the rivets are replaced with the springs in the whole structure, the damage around the rivets can be judged by checking the spring force.

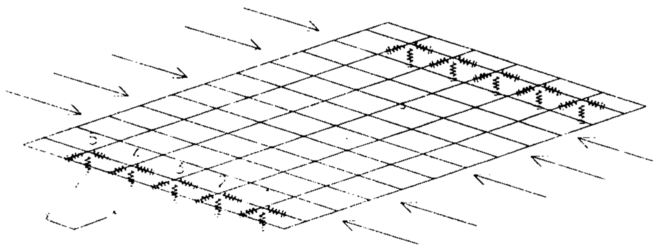

Fig.7

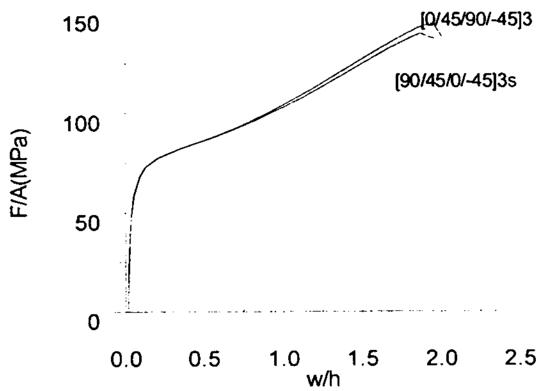

Fig.8

2.4 WHOLE STRUCTURE ANALYSIS Fig.7 presents the model of a whole structure, where the rivets are replaced by the X、Y、Z-spring. The stiffener is replaced by the "rigid bar" mentioned earlier. Compression force is applied on both the ends of the plate until the plate buckles and fails. The failure around the rivets is presented by the springs, while the failure other than the rivets is considered with Hashin criteria. Fig.8 shows the F/A-w/h curve of the plate stacking sequence $[0/45/90/-45]_{3s}$ and $[90/45/0/-45]_{3s}$, where 'w' represents the deflection of the center point of the plate, 'h' is the thickness of the plate, 'F' is the acting force, and 'A' is the section area of the plate. The plate of stacking sequence $[0/45/90/-45]_{3s}$ is discussed in this section.

When the buckling occurs (the acting force F/A is about 70 MPa) the center point start to raise out of plane. The force starts decreasing as F/A reaches about 140 MPa. Now we observe the change of the spring force, we find that the spring force is decreasing at the same time. The spring-force of some Z-springs decreases when the compression force decreases, while the X, Y direction does not. These decreasing Z-springs are near the center of the plate (numbered 2, 3, 4 in Fig.7) which indicates that the material around the rivets is damaged due to the Z-direction deflection, the defection is caused by the buckling of the plate. No failure occurs except the Z-spring force decreasing, that means that the failure around the rivet causes the total acting force to decrease, and makes the structure collapse at last.

3. EXPERIMENT

3.1 Preparation A series of experiments were performed to verify the numerical analysis. The dimension and the material of the specimens is the same as in numerical model. All the specimens were cured under a standard cycle. The laminates were fastened with aluminum stiffeners by rivets. The upper and the lower end of the plate are simply supported, the compression is applied on the upper edge while the lower edge is not moved. The experiment setup is shown in Fig.9, a laser displacement sensor is employed to measure the displacement of the center of the plate.

starts decreasing. This indicates that the material is damaged only in the Z direction.

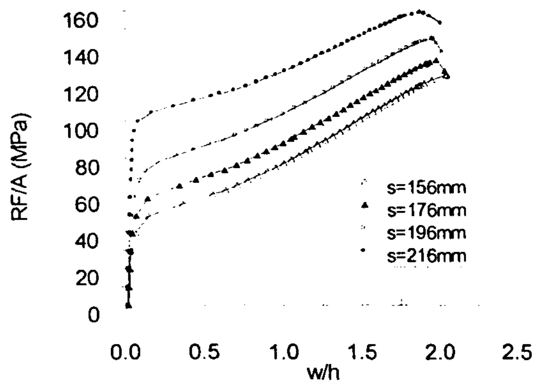

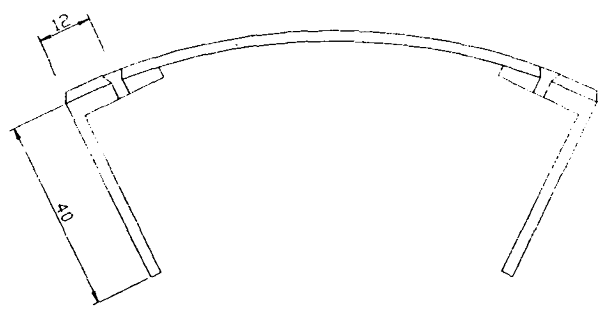

Fig.12 Fig.13

4.2 Curvature of the Plate The spring is applied in laminates with curvature (as shown in Fig.13), four cases are considered in this research. The chord length of the four cased are all 200mm, the curvature radius are 200mm (named as case I), 386mm (case II), 766mm (case III), and 1638mm (case IV) respectively. The buckling modes of these four cases are combining one semi-wave and three semi-waves , as shown in Fig.14), while the buckling mode of the plates is only one semi-wave.

Fig.15 presents the results of these four cases, the dashed line indicates the compression load versus the displacement of the center point (node a in Fig.14), while the solid line indicates the compression load versus the displacement of the node b. When the buckling mode is one semi-wave, the displacement of point a is higher than point b, while the displacement of point b is higher than point a when the buckling mode is three semi-wave.

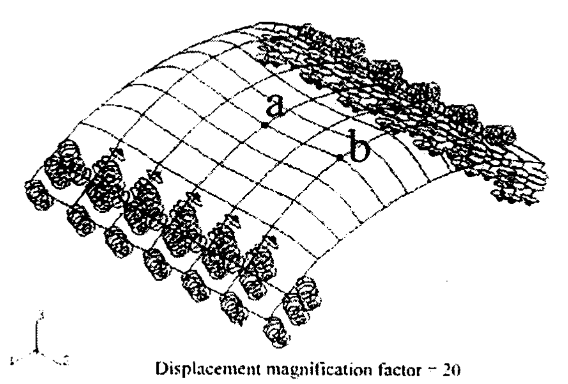

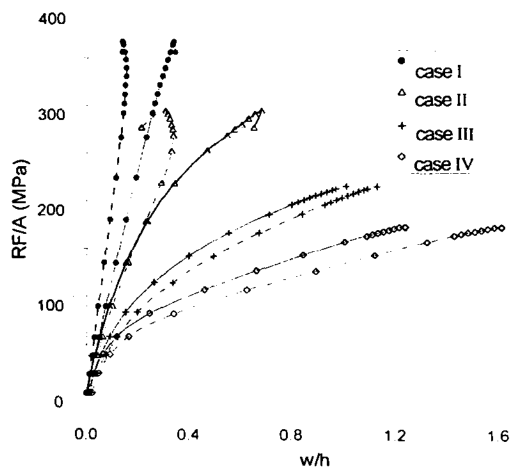

Fig.14 Fig.15

In case I and case II, the displacement of node b is higher than that of node a, the buckling mode is mostly three semi-waves. The higher the curvature, the smaller the displacement of center point. The failure load is also higher as the curvature increase. The failure appears around the rivet near the compressed edge, this can be seen from the decreasing force of the spring.

In case III and case IV, the displacement of node a is higher than that of node b, the buckling is mostly one semi-wave. The curvature of these two cases are small, their buckling behavior is similar to plate. However, the buckling load of plate is obvious, can easily be determined from the load-displacement curve, while the buckling load of case III and IV is not clear. This

7. Y. J. Lee, H. J. Lin, J. J. Lin " Numerical and Experimental Analysis on the Buckling Strength of Composite Materials Connected by Rivets (II) ". A Technical Report on the Project of the Development of National Defense, CS 80-0210-D-002-33(1991) (in Chinese)

8. Y. J. Lee, T. C. Her, J. J. Lin " Study on the Post -Buckling Behavior of Laminate Connected by Rivets ", the Master Thesis of National University of Taiwan(1996) (in Chinese)

9. Hashin Z., Failure Criteria for Uni-directional Fiber Composites, ASME J. Appl. Mech., 47, 329 (1980).

3.2 Results and Discussion Fig.10 and Fig.11 show the curves of stacking sequence $[0/45/90/-45]_{3s}$ and $[90/45/0/-45]_{3s}$ respectively. The results of the experiment is close to the numerical result in both cases, the failure mechanism is also similar. The main failure appears around the rivet near the forced end (numbered 4, 5 in Fig.7). This rivet takes the most compression force, so that the material around the rivet is damaged most. In numerical analysis, the spring force of the Y-spring near the forced end is the only one to decrease. This indicates that the failure of the material is around that rivet. Thus, the conclusion is exactly in accord with the result of the experiment.

In both the experiment and the numerical analysis, the failure load, failure mode, and the curve of the acting load are in concordant. From the above discussion, the experiments verify the validity of the numerical simulation.

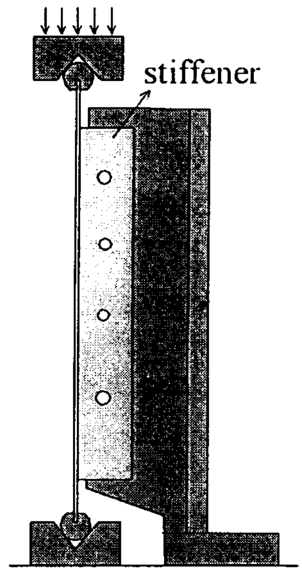

Fig.9

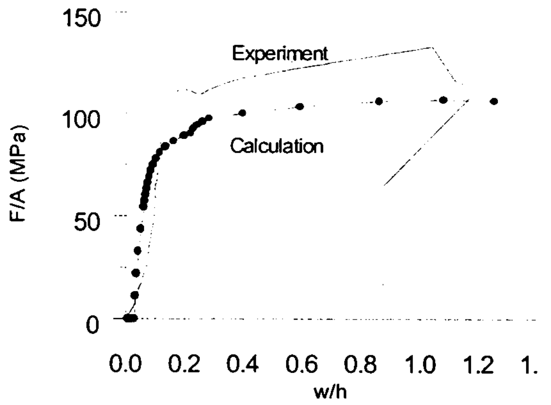

Fig.10

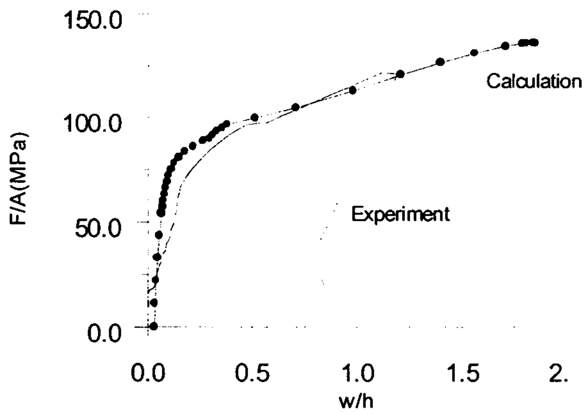

Fig.11

4. APPLICATION

Replacing the rivets with the springs makes it easier to analyze a whole plate. It is also convenient to observe the mechanic behavior around the rivets by the force-stretch curve of the spring. Through this method, the post buckling behavior of various composite plates can be investigated. In the following discussion, two parameters are studied, the width of the plate, and the curvature of the plate.

4.1 Width of the Plate Four cases are discussed, the span of the plate (as shown in Fig.1) s=156mm, s=176 mm, s=196mm, and s=216mm, note that Lb is not changed in these four cases. The ratio of length to width greatly influences the buckling behavior of the plate. The more the ratio, the higher the buckling load, this trend can be seen from Fig.12. The buckling modes of these four laminate are all one semi-wave.

In numerical analysis, the failure does not appear on the plate except the rivets. The breakage near rivets can be seen from the spring force. The X-, and Y-spring force of all these cases does not decrease, while the Z spring 2, 3, 4 (numbered in Fig.7) reaches the top and then